This is an open access article published under a Creative Commons Attribution (CC-BY) License, which permits unrestricted use, distribution and reproduction in any medium, provided the author and source are cited.

CHEMISTRY OF MATERIALS
Cite This: Chem. Mater. 2019, 31, 521−531
Article
pubs.acs.org/cm

Shaping Silica Rods by Tuning Hydrolysis and Condensation of Silica Precursors

Fabian Hagemans,* Ravi Kumar Pujala, Danisha S. Hotie, Dominique M. E. Thies-Weesie, D. A. Matthijs de Winter, Johannes D. Meeldijk, Alfons van Blaaderen,* and Arnout Imhof*

Debye Institute for Nanomaterials Science, Utrecht University, Princetonplein 1, 3584 CC Utrecht, The Netherlands

Supporting Information

ABSTRACT: We present the synthesis of colloidal silica particles with new shapes by manipulating the growth conditions of rods that are growing from polyvinylpyrrolidone-loaded water-rich droplets containing ammonia and ethanol. The silica rods grow by ammonia-catalyzed hydrolysis and condensation of tetraethoxysilane (TEOS). The lengthwise growth of these silica rods gives us the opportunity to change the conditions at any time during the reaction. In this work, we vary the availability of hydrolyzed monomers as a function of time and study how the change in balance between the hydrolysis and condensation reactions affects a typical synthesis (as described in more detail by our group earlier[1]). First, we show that in a "standard" synthesis, there are two silica growth processes occurring; one in the oil phase and one in the droplet. The growth process in the water droplet causes the lengthwise growth of the rods. The growth process in the oil phase produces a thin silica layer around the rods, but also causes the nucleation of 70 nm silica spheres. During a typical rod growth, silica formation mainly takes place in the droplet. The addition of partially hydrolyzed TEOS or tetramethoxysilane (TMOS) to the growth mixture results in a change in balance between the hydrolysis and condensation reaction. As a result, the growth also starts to take place on the surface of the water droplet and thus from the oil phase, not only from inside the droplet onto a silica rod sticking out of the droplet. Carefully tuning the growth from the droplet and the growth from the oil phase allowed us to create nanospheres, hollow silica rods, hollow sphere rod systems (colloidal matchsticks), and bent silica rods.

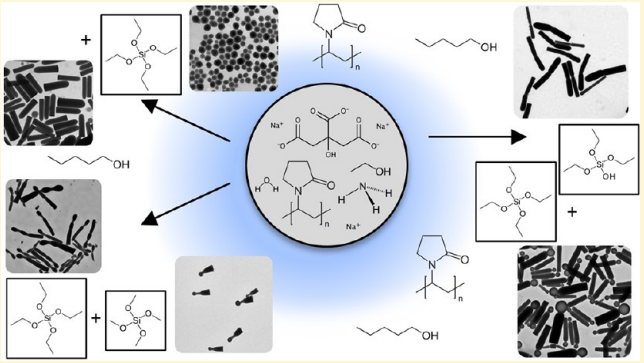

INTRODUCTION

Colloids are promising building blocks in materials synthesis because of the possibility to control their size, anisotropy, and surface properties.[2−4] Recent developments to exploit the particle shape have led to several interesting applications in areas ranging from biology to materials science. Investigations of such anisotropic colloids resulted in the development of novel multifunctional and advanced materials.[5−10] Anisotropic colloidal particles have attracted a lot of attention because of their widespread applications in emulsion stabilization, optical displays, imaging, drug delivery, and active materials.[11−14] Recently, great improvements have been made in the development of novel synthetic techniques to introduce anisotropy in colloids with the goal of attaining various novel complex morphologies.[15−22] The anisotropy can be geometrical, chemical, or both. However, the synthesis of geometrical or chemical anisotropic particles is far more difficult than the synthesis of spherical particles. Tuning the properties of the shape and polydispersity of anisotropic particles during growth is a major challenge.

Different strategies have been developed to produce anisotropic particles which allow the synthesis of anisotropic colloids and nanoparticles with a narrow size distribution. Typically, colloidal particles are produced using a bottom-up process, leading to spherical particles that can consist of many different materials. Instead of adding materials from all sides at an equal rate, one can sometimes add material one-sided. Anisotropic addition of material results in particles that can be anisotropic in chemistry and/or shape. A well-known example is the different reactivity of facets on nanocrystals.[23] Some facets grow at a higher rate than others; capping agents and surfactants can be used to further tune this process. Different growth rates of crystal facets capped with organic ligands were found in the synthesis of, for example, CdSe nanorods, CdSe nanodisks, and gold nanorods.[23,24] Gold nanorods are synthesized in the presence of CTAB which interacts specifically with certain facets of the growing gold nanorod.[24] A powerful way to remove or add building blocks to shape colloidal particles in an asymmetric fashion is by making use of the different properties of a continuous phase and a dispersed phase. When a colloidal particle is adsorbed to an interface, one side is exposed to the dispersed phase and the other side

Received: November 2, 2018
Revised: December 14, 2018
Published: December 15, 2018

Downloaded via UTRECHT UNIV on January 29, 2019 at 12:50:17 (UTC).
See https://pubs.acs.org/sharingguidelines for options on how to legitimately share published articles.

to the continuous phase. In this way, one can remove material from one side only and reshape isotropic particles into anisotropic shapes.[25] Furthermore, instead of removing material, one can also add functional groups to create Janus particles.[26−31] Although these synthesis routes result in many new shapes of particles, they are based on a 2D method. These synthesis methods typically result in small yields. In order to obtain a larger amount of particles for self-assembly studies, 3D bulk growth methods are more viable. A well-known synthesis route to prepare anisotropic particles is by swelling a polymer seed particle and the subsequent formation of a protrusion on the polymer seed particles. The stress on the cross-linked polymer network that arises due to swelling of the particles with the monomer presses out a liquid monomer droplet anisotropically.[32−37]

A recently developed synthesis route by our group that makes use of the anisotropic addition of the building blocks is the synthesis of silica rods,[1,38] which can also be fluorescently labeled[39] for quantitative real space studies.[40] These silica rods grow from a polyvinylpyrrolidone (PVP), sodium citrate, ethanol, and ammonia-loaded droplet that is rich in water and dispersed in an oil phase (usually pentanol) which contains PVP as well. The silica precursor requires water (1:4) for the hydrolysis reaction, while it also catalyzes the release of water (1:2) in the condensation reaction.

The typical amounts of the precursors used in the synthesis of silica rods (L = 1600 ± 160 nm, D = 260 ± 64 nm) are displayed in Table 1. These conditions will be referred to as a "standard" synthesis, as they have been used by many authors.

Table 1. Amount of Reagents Used in a "Standard" Synthesis of Silica rods[a]

component	amount	amount (moles)
pentanol	10.0 mL	92 mmol
PVP	1.0 g	25 μmol
ethanol	1.0 mL	17.4 mmol
water	0.280 mL	15.5 mmol
sodium citrate (0.17 M)	0.067 mL	11.4 μmol sodium citrate, 3.7 mmol water
ammonia (25%)	0.225 mL	1.7 mmol ammonia, 9.4 mmol water
TEOS	0.10 mL	0.45 mmol

[a]After the addition of TEOS, the reaction was continued for 24 h.

The mechanism behind the rod growth has been discussed in the literature by several authors. Zhang et al. initially proposed a form of templated growth.[38] They proposed that silica was deposited onto a rodlike PVP−water−gold aggregate. However, we showed by using cryo-transmission electron microscopy (TEM) that a droplet with a high concentration of PVP is present on one end of the growing rod.[1] The rod was found to be growing unidirectionally from the PVP−water droplet. Furthermore, the presence of the gold nanoparticles is not required for rod growth. We proposed that the ion citrate was responsible for the stabilization of the droplet.[1,41] Zhang et al. categorized this mechanism of growth as a solution−solution−solid mechanism similar to a vapor−liquid−liquid mechanism.[42,43] Later, Yu et al. proposed that the interaction between citrate and PVP likely induces the phase separation of alcohol and water and thus the formation of the droplet.[44] Murphy et al. suggested that a competition between silica rod growth from an attached watery droplet[1] and a templated growth mechanism (silica deposition onto precipitated citrate) was likely to occur.[45]

Temperature influences the rod growth significantly.[46] Changing the temperature during the synthesis resulted in a step change in the width of the silica rods, as found by Datskos and Sharma[47] Yang et al. found that by using the same temperature step, a bent segment was formed instead of a straight segment. In this way, bent silica rods with a tunable angle could be produced.[48] The origin of this difference in the outcome of the synthesis remains unclear and will be discussed in this paper.

In this paper, we focus on the relation between the rates of hydrolysis and condensation and the morphology (matchstick, hollow parts, bent rods) of the rodlike particles formed. We start with the conditions necessary for the formation of water-rich droplets in a homogeneous pentanol phase, which originates from the interaction of PVP with citrate and water. We show that the emulsion is unstable in the long run; this is caused by the non-zero solubility of water in the pentanol phase. The finite solubility of water and ammonia in the pentanol phase has a great effect on the hydrolysis and condensation rates in the pentanol phase as compared to the same processes taking place in the water-rich phase. The effect of hydrolysis in the pentanol phase on the rod growth was examined by pre-hydrolyzing a certain percentage of the monomer tetraethoxysilane (TEOS) and adding this at the beginning or during the rod growth. We show that by playing with this amount of hydrolyzed silica precursors, and thus the ratio of hydrolysis versus the condensation reactions, silica condensation and deposition can also be made to occur directly from the oil phase onto the water phase, creating hollow silica sections, conditions that were described in other papers as well.[48−51] We will explain why these differences reported are due to differences in the amount of (pre)-hydrolyzed silica precursors present. We also influenced the hydrolysis and condensation rates by using mixtures of tetramethoxysilane (TMOS) with TEOS to grow the rods. These changes were found to bring about silica deposition onto the outer surface of the water droplets, resulting in a large variety of new shapes of silica particles. These include rods with a hollow sphere at their tip, bent rods, and bat-shaped particles. Energy-dispersive X-ray spectroscopy (EDX) was used to analyze the hollow structures formed and clarify the mechanism.

RESULTS AND DISCUSSION

Rod Growth Mixture. To better understand the mechanism for rod growth, we first examined the conditions for the formation of a separate water phase by examining the reagent mixtures for a change in turbidity upon the addition of each of the components. The water-rich emulsion droplets, containing PVP, citrate ions, ammonia, and pentanol, which are dispersed in a pentanol-rich oil phase, are the starting points of rod growth. The system described in Table 1 will be studied in detail.

The solubility of water in pentanol is 0.086 g/mL and of pentanol in water is 0.024 g/mL for T = 293 K.[52,53] Therefore, small amounts of water will mix completely with the pentanol until the saturation value has been reached. This could be clearly observed macroscopically, when a solution of 1.0 g PVP in 10.0 mL pentanol was mixed with 0.28 mL water. A transparent and well-mixed solution was the result. Also, upon the addition of 0.225 mL ammonium hydroxide to 10.0 mL

DOI: 10.1021/acs.chemmater.8b04607
Chem. Mater. 2019, 31, 521−531

pentanol and 1.0 g PVP, a homogeneous mixture was formed. However, upon the addition of 0.067 mL sodium citrate (0.17 M) to the pentanol, a change in the turbidity was observed. We expect that the citrate ion interacts with the PVP molecules and small droplets of polymer and citrate ions, swollen with water, are formed. Figure 1 shows the macroscopic behavior; in each container, one of the components is added. In case a dispersed phase is soluble in the continuous phase, Ostwald ripening of the water droplets can occur; large droplets grow at the expense of smaller droplets reducing the total interfacial energy. Because of the non-zero solubility of water in pentanol, this also happens in our emulsion as shown in Figure SI1, where we show using dynamic light scattering that the slow increase in droplet size confirms this behavior.

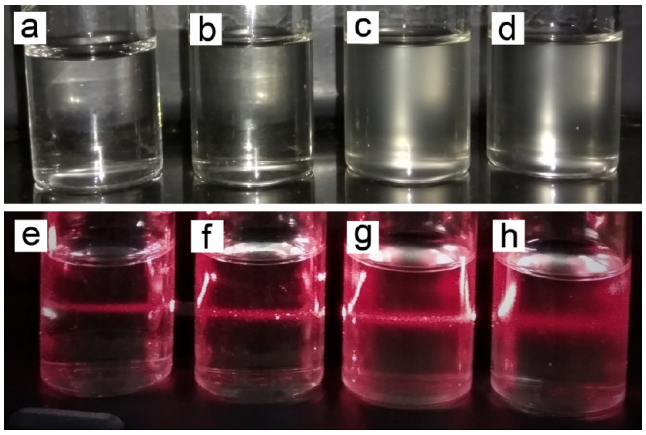

Figure 1. Macroscopic observations for various combinations of the reagents. (a,e) 10.0 mL pentanol, 1.0 g PVP, 0.28 mL water (b,f) 10.0 mL pentanol, 1.0 g PVP, 0.28 mL water, 0.225 mL ammonia (c,g) 10.0 mL pentanol, 1.0 g PVP, 0.28 mL water, 0.067 mL sodium citrate (0.17 M) (d,h) 10.0 mL pentanol, 1.0 g PVP, 0.28 mL water, 0.225 mL ammonia, 0.067 mL sodium citrate (0.17 M).

After the "standard" rod growth had completed, we noticed that besides the growth of silica rods, a population of silica spheres is also always formed using our "standard" growth conditions, which were not mentioned in the literature until now. These spheres, with an average diameter of 70 nm, were considerably smaller than the width of the silica rods; see Figure 2. They are routinely lost after one or two washing steps by centrifugation. It is likely that these particles are formed by the nucleation and growth of silica oligomers in the continuous phase. Because of the non-zero solubility of water and ammonia in pentanol, hydrolysis and even condensation take place from the continuous phase onto the water droplet and/or completely in the oil phase (Stöber process). The amount of spheres will strongly depend on the growth conditions as it is well known for Stöber growth that the size (and thus the number and surface area) of the spheres will strongly depend on the ionic strength, amount of water and ammonia, and dielectric constant, which are changed by changing the reaction conditions. Depending on the growth conditions of the rods, the growth of these particles will also be altered. Hence, the size, number, and surface area of these particles should vary with the exact reaction conditions, and their influence on this fraction should be studied in detail in further work. We believe that the spherical particles found in the various cases described by our group[1] are these small silica spheres which grew larger in cases where rod growth did not take place. For the "standard" synthesis of silica rods, in total, 114 mg of silica was collected after centrifugation, 50% (w/w) was found to be in the form of nanospheres, and 50% (w/w) was found to be rod-shaped. In this experiment, we studied the influence of several reaction parameters on the rod fraction.

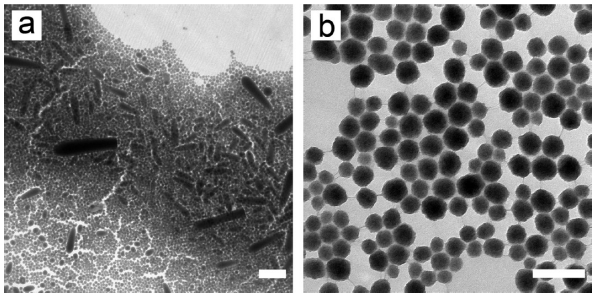

Figure 2. (a) Complete sediment of a "standard" synthesis of silica rods (L = 1600 ± 160 nm, D = 260 ± 64 nm) shows a fraction of silica spheres and a fraction of silica rods. A zoomed-in TEM image of the silica spheres that were found is shown in panel (b). Scale bars indicate (a) 1 μm and (b) 200 nm.

Effect of Partial Pre-Hydrolysis of TEOS. The locations where hydrolysis and condensation of TEOS take place in the two-phase system have a great effect on the final particle structure and composition. Fortunately, we can influence the amount of hydrolyzed TEOS independently by a partial pre-hydrolysis step of TEOS before it is added to the reaction mixture. A first indication that this has an effect was found when we used TEOS that had been exposed to air regularly for 1.5 years. Similar effects are also visible in images and are speculated about in several papers as well.[44,48−50] Using this precursor in the synthesis of silica rods resulted in particles that had a small hollow sphere attached to the tip of the rod where the growth started; see Figure 3a. On the contrary, TEOS from a newly opened bottle resulted in silica rods that did not have this modification. This remarkable effect can only be explained by the hydrolysis and possibly partial condensation (no units that scatter light were visible) of TEOS over time. When opening the bottle regularly to air, atmospheric water can be adsorbed from the air into the TEOS solution. Over long periods of time (days at least, as no catalyst is present), a part of the TEOS molecules can become hydrolyzed and partially condensed. Once the molecules have diffused toward the water droplet and crossed the water−pentanol interface, condensation can take place immediately. This results in the condensation of TEOS at the interface of the water droplet and therefore the coverage of the droplet interface. As only part of the TEOS is pre-hydrolyzed, the silica deposition from the oil phase will diminish over time, after which "standard" growth resumes as for pure TEOS. Apparently, the continued "regular" hydrolysis and condensation of TEOS on the inside of the hollow spheres slowly presses out the droplet. [More evidence for this mechanism is discussed below with the results on the elemental analysis and focused ion beam (FIB) scanning electron microscopy (SEM)/TEM].

To confirm that the spherical hollow shell (wrt silica content) is caused by the partial pre-hydrolysis of added TEOS, we pre-hydrolyzed fresh TEOS deliberately and added this to our "standard" (Table 1) synthesis procedure. In this case, TEOS was partially hydrolyzed by mixing TEOS (11 mL) with water (0.8 mL) and a low concentration of hydrochloric acid (21.0 μL, 0.2 mmol). The molar ratio TEOS/H_2O was

DOI: 10.1021/acs.chemmater.8b04607
Chem. Mater. 2019, 31, 521−531

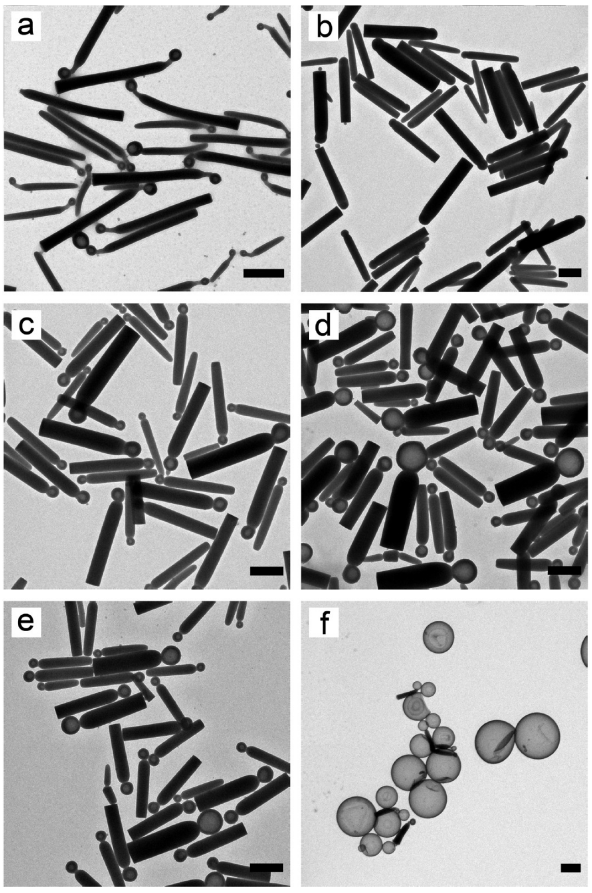

Figure 3. Addition of a small quantity of partially pre-hydrolyzed TEOS [(b), 2.3% (v/v_{TEOS}), 0.03 mmol] results in rods with a hollow sphere attached comparable to the rods formed when using TEOS that had been in contact with air regularly (a). The deformation is caused by the presence of hydrolyzed TEOS. However, with increasing volume fraction [see panel (c) 7% (0.09 mmol), (d) 14% (0.18 mmol), and (e) 28% (0.36 mmol)], the diameter of the spherical and hollow segment increases. For high concentrations of partially pre-hydrolyzed TEOS, >75% (f), we find mostly hollow spheres without a rod attached. Scale bars indicate 1 μm.

1:1. In acidic media, the hydrolysis of TEOS is sped up.[55] Initially, water did not mix well with TEOS. However, as the hydrolysis reaction proceeded, partially hydrolyzed TEOS became more hydrophilic. After 10 min of hydrolysis, no more phase separation between TEOS and water−ethanol was observed. In order to change the conditions of growth for the rods, we added a small quantity of partially hydrolyzed TEOS, which contained water (12.8 μmol) and HCl (0.057 μmol) per 0.01 mmol partially hydrolyzed TEOS, together with fresh TEOS to the reaction mixture keeping the number of moles of the silica precursor constant.[55] The amount of extra water added is much less than the total amount of water (28.6 mmol) present in the system. Also, the amount of HCl is much smaller than the amount of NH_3 (1.7 mmol). The degree of hydrolysis was varied by changing the ratio between fresh TEOS and partially hydrolyzed TEOS. The resulting particles synthesized at volume fractions ($v_{hydrolysed\ TEOS}/v_{TEOS}$) of 2.3% (0.03 mmol of hydrolyzed TEOS), 7% (0.09 mmol), 14% (0.18 mmol), and 28% (0.36 mmol) are shown in Figure 3b−e, respectively. A comparable change in the shape of the particle is observed as for old TEOS. At low concentrations [2.3% (v/v), 0.03 mmol], a small sphere was found at the tip of the rod. This sphere became larger and hollow as the ratio of partially pre-hydrolyzed TEOS to TEOS was increased. At a volume fraction of 7% (0.09 mmol) and higher, a complete hollow sphere was found at the tip of the rod. Depending on the ratio, the size of the sphere increased, the thickness of the sphere shell decreased and the rod length also decreased slightly. Note also in all cases the strong correlation between the sphere and rod diameter. At concentrations of 75% (1 mmol) and higher, only hollow spheres were found, as can be seen in Figure 3f. The image mainly shows larger hollow shells, as the smaller hollow shells were lost in centrifugation steps. The absence of any rods indicates that the droplets were fully covered with silica and that rod growth was prohibited.

These results clearly show that the spherical segment at the tip of the rods was caused by the partial hydrolysis of TEOS. Apparently, there is a competition between formation of a shell by prehydrolyzed TEOS arriving from outside the droplet and formation of a rod from silica formed inside the droplet. We believe that this may also explain some similar shapes observed in the literature,[48−51] where the spherical segment at the tip of the rod was observed but was not always remarked upon and/or explained. The connection between the formation of the hollow tips or head on the rods (matchstick shape) and hydrolyzed TEOS was recently suggested by Sharma as well[49] in a recent review.

Initial Stages of Hollow Sphere-Tipped Rod Growth. The mechanism of growth of the hollow sphere attached to the tip of the silica rods became more apparent when taking early samples of the growing silica rods. Figure 4a−c shows the initial segment of the silica rods grown after 5, 10, and 20 min, respectively. After 5 min of growth, a hollow sphere was found with an opening on one side. Further growth of the silica rods, after 10 min, resulted in the narrowing of this opening. Furthermore, the growth seemed to continue anisotropically. After 20 min of growth, a neck had formed between a hollow spherical shell and a segment of a solid rod (Figure 4c).

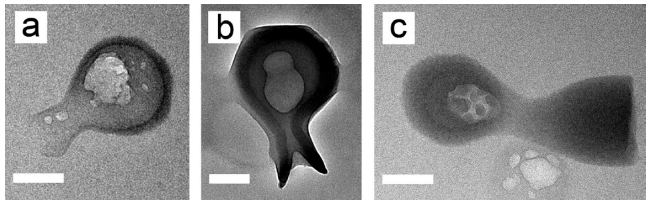

Figure 4. Growth of silica rods, with 14% partially pre-hydrolyzed TEOS present, quenched by centrifugation and redispersion after (a) 5, (b) 10, and (c) 20 min of growth. The neck became narrower with time due to the growth of silica on the inner side of the particles. The scale bar indicates 100 nm.

Composition of the Particles. To further elucidate the origin of the hollow spheres attached to the rods, we also studied the structure of the rod using FIB−SEM. For this, we used the sample shown in Figure 3d. Using a FIB beam, we opened the tip of the rod and studied the interior of the particle using SEM. The SEM image in Figure 5b clearly shows that the inside of the spherical part is indeed hollow and could have contained a part of the emulsion droplet. To confirm the encapsulation of (part of) the emulsion droplet, we mapped the presence of sodium, chlorine, silicon, and oxygen using EDX (see Figure 5c−f). Sodium was added to the reaction as a counter ion of citrate and is expected to be mainly present in the droplet, as shown by Datskos et al. in 2016.[56] Therefore, if

DOI: 10.1021/acs.chemmater.8b04607
Chem. Mater. 2019, 31, 521−531

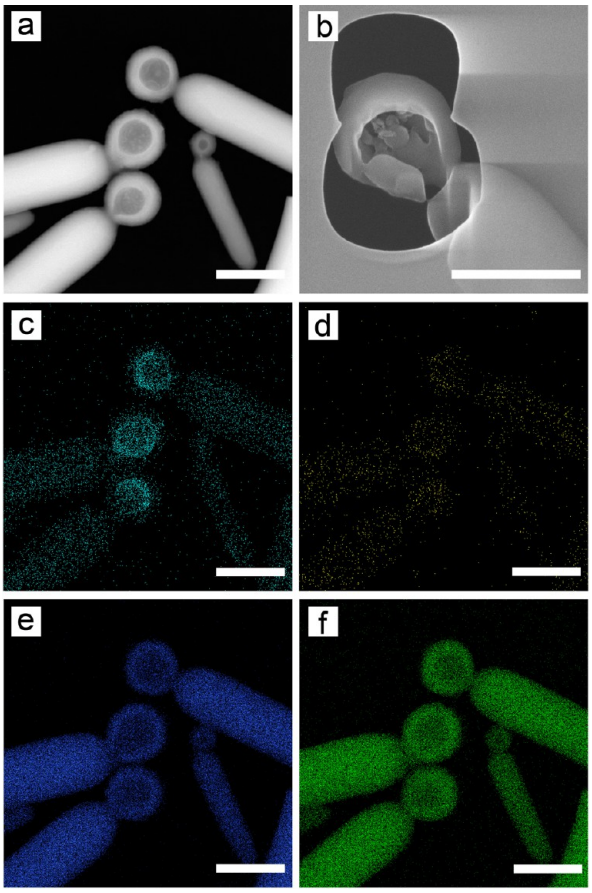

Figure 5. (a) Scanning TEM image of silica rods prepared using 14% (0.18 mmol) of partially pre-hydrolyzed TEOS. (b) SEM image of a FIB cut through the spherical section of a silica rod displaying that the tip of the rod is at least partially hollow. Panels (c–f) show the EDX map of sodium, chlorine, silicon, and oxygen, respectively. The tip of the rod contained an increased concentration of sodium, which can only originate from sodium citrate that was dissolved in the PVP–water droplet. Scale bars indicate 500 nm.

part of the droplet got encapsulated during growth, a fraction of sodium should be found left behind inside the hollow sphere. The EDX map of these silica rods with a hollow sphere attached indeed shows that there is a higher concentration of sodium in the center of the sphere and a lower concentration throughout the straight segment. When compared to the silicon map, it becomes clear that the sodium is located mainly on the inside of the hollow sphere and not spread through the silica material. This clearly shows that during the growth, part of the water droplet, containing sodium citrate and PVP, got encapsulated. However, the hollow sphere is likely not caused by the templated growth onto a citrate crystal, as suggested earlier by Murphy et al.;[45] the concentration of sodium in the hollow segment seems too low for it to be filled with a sodium citrate crystal. This result shows a promising route toward encapsulating water soluble molecules or particles specifically on one side of the rod. It also provides mechanistic insight in recent syntheses of silver-head, titania-head, manganese oxide-head, and iron oxide-head "matchstick" rods.[41,57−60] The presence of sodium ions in the hollow segment was also found in cryo-EDX–SEM experiments; see Figure SI2. Here, the growing particles were frozen using liquid nitrogen and subsequently analyzed under cryogenic conditions.

Delayed Addition of Pre-Hydrolyzed TEOS—Bent Rods. To investigate the effect of partially hydrolyzed TEOS on the continued growth of silica rods, we added partially pre-hydrolyzed TEOS at intermediate stages during the synthesis. To this end, we started a silica rod synthesis using the "standard" growth procedure, and after 2 h added an amount of partially hydrolyzed TEOS to the reaction mixture. Typical TEM images are shown in Figure 6. At low concentrations,

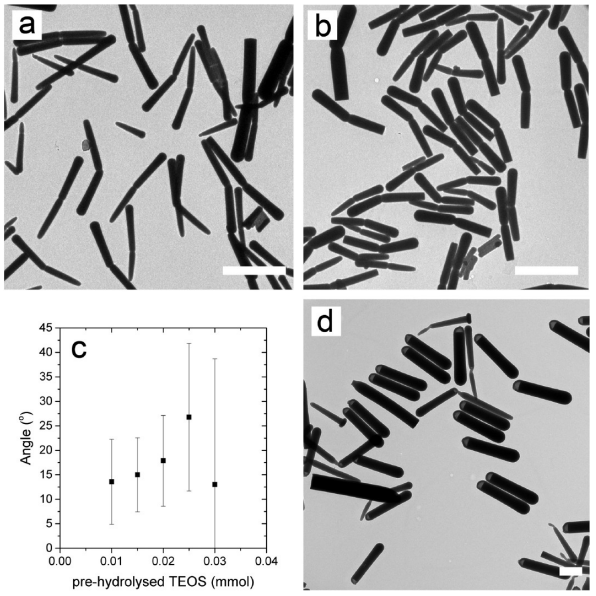

Figure 6. Bent silica rods prepared using partially pre-hydrolyzed TEOS added after 2 h of growth. At low concentrations [(a), 2.3% (v/v), 0.01 mmol], the rods bend only slightly, but with increasing concentration [(b), 4.6% (v/v), 0.02 mmol], the bend angle increases as shown in (c). For 1.0 mmol of partially hydrolyzed TEOS, the droplet got completely encapsulated by a thin shell of silica (d). The error bars in (c) indicate the spread in the angle (standard deviation of the size distribution) and not the error in the average. Scale bars indicate 1 μm.

2.3% (v/v) (0.01 mmol) of partially pre-hydrolyzed TEOS, a small bend was observed in the middle of the rod. However, at higher concentrations, we observed that a larger bend appeared, together with a decrease in diameter (by 195 nm), at the moment of the addition. The length of this constriction did not increase significantly with the concentration of partially pre-hydrolyzed TEOS. Beyond the bend growth continued as "normal" for an undisturbed rod growth in a straight fashion, but with an only slightly smaller diameter (45 nm decrease). Upon increasing the amount of partially hydrolyzed TEOS that was added to the growth mixture, the average angle of the bend in the silica rods increased. Figure 6c shows the dependence of the mean bend angle on the concentration of hydrolyzed TEOS. Interestingly, at concentrations of 75% (v/v) (1.0 mmol) of added pre-hydrolyzed TEOS (together with 1.28 mmol water and 5.7 μmol HCl), the droplet on most particles got completely encapsulated, and rod growth stopped as a result (Figure 6d). On the basis of our results, we think that it is likely that the bending of the silica rods, observed by Yang et al.,[48] is also caused by the presence of an amount of pre-hydrolyzed TEOS. However, as the method of Yang et al. also includes a heating step, potentially the method of heating could influence the rate of silica growth and as such have a comparable effect.

DOI: 10.1021/acs.chemmater.8b04607
Chem. Mater. 2019, 31, 521−531

TMOS Addition. *Initial Addition of TMOS.* The degree of hydrolysis of TEOS has an important effect on the morphology of the growing silica rods as followed from the previous sections. However, as mentioned in the previous methods, the concentration of water and the pH were slightly altered by the addition of pre-hydrolyzed TEOS as well, as the solution added also contained water and HCl. The hydrolysis rate can also be tuned without having to change the water concentration, by replacing the ethoxy groups by methoxy groups. The use of TMOS will increase the hydrolysis rate, without the use of a pre-hydrolysis step. It is well known that the hydrolysis rate of alkoxysilanes decreases with the chain length of the alkoxy group. In other words, TMOS has a higher hydrolysis rate than TEOS. The use of TMOS allowed us to study the effect of the hydrolysis rate on the rod growth separately from the effect of water on the rod growth.

To investigate the effect of the hydrolysis rate on the rod growth, we added TMOS and TEOS in various ratios to the growth mixture directly at the start of the synthesis. TEM images of these particles are shown in Figure 7. For all concentrations of TMOS, it was found that, as before, a hollow tip was formed, followed by a segment of significantly reduced diameter. Later on, the diameter increased again to the regular diameter found for silica rods (~300 nm). With increasing molar fraction of TMOS, this thinner segment increased in length and became less straight. At a molar amount of 0.39 mmol TMOS, the rod did not increase to the diameter found for silica rods grown using the "standard" procedure.

Delayed Addition of TMOS. The delayed addition of TMOS to the "standard" rod growth mixture also resulted in rods with a thinner section but further down the length of the rod (Figure 8a,b), as expected. After a short time, the diameter of the rod returned to its original size. The length of this section was found to correlate with the concentration of TMOS. More TMOS led to a longer thin segment, while its diameter was not affected. Besides the decrease in diameter, we also observed that the particles bent slightly after the addition of TMOS, and more so when the concentration was increased. The bend angle is shown in Figure 8c as a function of the TMOS amounts added. For an amount of 0.091 mmol or higher, the droplet got completely encapsulated for the majority of particles (results not shown).

At 0.068 mmol of TMOS, a hollow segment was found in the section that was grown directly after adding the extra precursor. This hollow section is likely caused by the increased concentration of silicic acid, leading to an increase of the condensation of silica onto the water droplet from the pentanol phase as described in the previous section. Because the diameter of the particles soon returned to almost its original size (with a 108 nm decrease), we thought it would be interesting to know what would happen upon the addition of a second amount of TMOS. Interestingly, the diameter decreased again upon the addition of new TMOS. However, the diameter of the rod did not return back to its original diameter (not shown). We explain this by the lowered

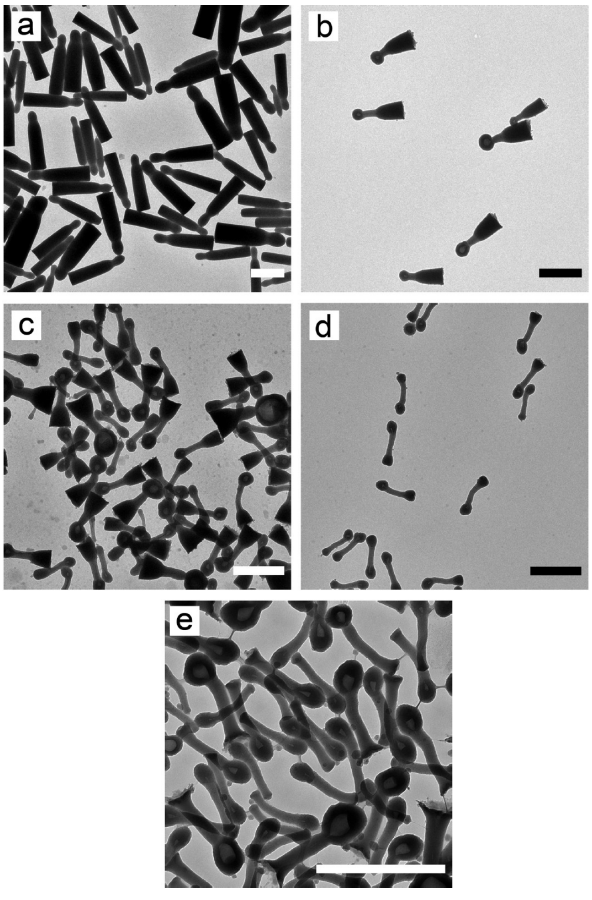

Figure 7. Silica rods grown with an increasing amount of TMOS. For a molar additions of (a) 0.087 mmol TMOS, we find that a small hollow silica shell is formed at the tip of the rod. Upon increasing the molar fraction to (b) 0.217 mmol TMOS, a thin hollow neck appeared in between the spherical head and the rod. With increasing molar fraction, the length of the hollow neck increased and the length of the rod part decreases. Typical TEM images of these particles are shown in (c) 0.30 mmol TMOS, (d) 0.35 mmol TMOS, and (e) 0.39 mmol TMOS. Scale bars indicate 1 μm.

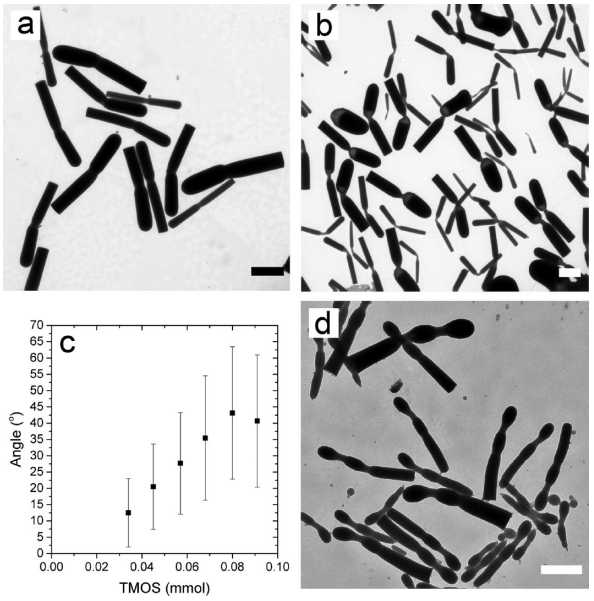

Figure 8. Bent silica rods prepared using TMOS, added after 2 h of growth. At low concentrations of TMOS [(a), 0.034 mmol] the rods bent slightly, with increasing concentration [(b), 0.068 mmol], the bend angle increases as shown in (c). The error bars indicate the spread in the angle (width of the size distribution), two sequential additions of a mixture of TMOS (0.068 mmol), and TEOS (0.087 mmol) are shown in (d). Scale bars indicate 2 μm (a,b) and 1 μm (d).

DOI: 10.1021/acs.chemmater.8b04607
Chem. Mater. 2019, 31, 521−531

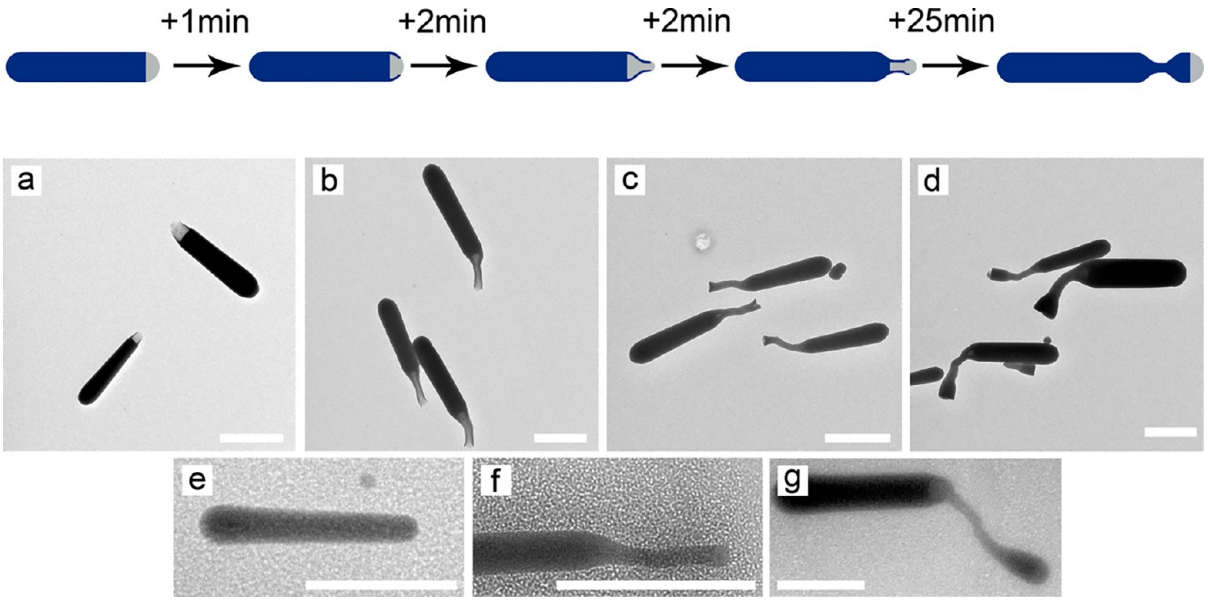

Figure 9. (a–d) TEM and (e–g) cryo-TEM images of intermediate stages in the synthesis of bent silica rods, after 2 h of initial growth. A hollow segment can be found directly after the addition of 0.091 mmol TMOS. (a) 1 min of growth after addition, (b) 3 min of growth, (c) 5 min of growth, and (d) 30 min of growth. Cryogenic samples of the growth mixture after (e) 1 min of growth and (f) 5 min of growth show that the droplet is spread over the long hollow tube and the deposition of silica from the oil phase is greatly enhanced. Finally, (g) 30 min after TMOS addition, the rod and droplet diameter increased. Scale bars indicate 1 μm.

concentration of TEOS. At the moment of addition, the TEOS concentration has decreased so much that there was no competition between the two reagents. However, if together with TMOS (0.068 mmol) a small amount of TEOS (0.087 mmol) was also added, the diameter of the rod did go back to its original size (Figure 8d). In this case, TMOS ran out before TEOS.

Intermediate Stages of Bend Formation. The mechanism behind this growth becomes more apparent if we look at intermediate stages in the synthesis. First, we studied the segmented growth of silica rods by the delayed addition of 0.068 mmol TMOS. Silica rods were first grown for 2 h following the "standard" reaction scheme, then TMOS was added, and the growth was followed by taking TEM images of samples withdrawn at various times (Figure 9a–d). At first, after 1 min of reaction time after addition, a small layer of silica had formed at the droplet interface, but the droplet was not fully covered by the silica layer. As the growth continued, a hollow tube formed with a diameter smaller than the original rod. After 5 min of growth, the hollow tube appears to have filled with material (compare Figure 9b,c). After 30 min of growth, the diameter of the particles had increased. Cryo-TEM images (Figure 9e–g) taken at the same times show the same process, but with the emulsion droplets preserved. The roundedness of the growing tip evidences the presence of the droplet there: changes in the rod diameter follow changes in the droplet size. The sequence of events, partial coverage of the droplet, thin segment formation, and return to regular rod growth are comparable to the case of hydrolyzed TEOS addition at the start of a synthesis (Figure 4).

High Hydrolysis Rate—Titanium Alkoxide. Titanium isopropoxide has a much higher hydrolysis rate than tetraalkoxysilanes.[61] Therefore, the nucleation and growth is expected to be highly influenced. Indeed, upon adding 0.45 mmol titanium (IV) isopropoxide or 0.45 mmol titanium (IV) isobutoxide precursor to the general growth mixture (Table 1), instead of 0.45 mmol TEOS, we found that the formation of non-rod-shaped particles in the oil phase was greatly increased, whereas growth from the droplet was not present anymore. The precursor had to diffuse through the oil phase, which contained water, to the water droplet. Because of the much higher hydrolysis rate, the titania precursor was apparently fully hydrolyzed before it could reach the water droplets. This resulted in a higher concentration of hydrolyzed precursor molecules in the pentanol phase and the subsequent condensation reaction in the presence of ammonia. Also, changing pentanol to decanol, which has a much lower solubility for water, did not induce the growth of rods.

Mechanism. The mechanism we propose with respect to morphology changes of a "standard" rod synthesis when hydrolyzed amounts and reaction of silica precursor rates are changed is as follows. The preparation of silica rods starts with the nucleation of droplets. The injection of an aqueous solution of sodium citrate into pentanol–PVP, and the mixing by shaking leads to the formation of PVP–citrate-rich droplets. After the out-of-equilibrium formation of droplets with a certain size and polydispersity, Ostwald ripening on the time scale of hours led to emptying of smaller droplets into larger ones. This process also explains the diameter decrease for a fraction of the thinnest rods, some of which lose the droplet completely during the rod growth, which generally takes hours to complete. Nucleation of the rod takes place in the water droplet because of the increased concentration of ammonia in the droplets with respect to the pentanol phase. A silica particle nucleates in the water-rich droplet phase, adsorbs to the interface, and starts to grow inhomogeneously from then onward. Further growth takes places from inside the droplet because the concentration of water is the highest there. However, these reactions do not solely take place in the water droplet, but also in the pentanol phase. Because of silica growth in the pentanol phase, a population of silica spheres was also found, but is readily removed in subsequent cleaning

DOI: 10.1021/acs.chemmater.8b04607
Chem. Mater. 2019, 31, 521–531

steps. As much as 50% silica yield ended up as spheres, but this yield was unfortunately not checked for all other conditions investigated when different rod morphologies were found. Furthermore, deposition of silica directly from the pentanol phase onto the growing rod also occurs. This leads to the thin shell of more condensed silica as reported on by our group earlier.[54] The balance between silica deposition from the oil phase on the outside of the water-rich droplet and from inside the water phase is determined by the water concentration, the ammonia concentration in the pentanol phase, the degree of hydrolysis of the precursor and its hydrolysis and condensation rate. For a "standard" rod growth (Table 1), the balance between silica deposition in the oil phase and in the water phase is also highly influenced by the degree of hydrolysis of the initially added TEOS. When 0.18 mmol of pre-hydrolyzed TEOS is added, the rate of silica deposition from the oil phase directly onto the water interface will increase. This encapsulates part of the droplets, so that the resulting rods have an initial hollow sphere at the tip of the silica rods and a matchstick-like shape. Such rods could also be synthesized by using aged TEOS, which is also partly hydrolyzed, and TMOS, which hydrolyzes much faster. The composition of the hollow sphere at the tip of the rods clearly reflects the composition of the initial water droplet as demonstrated by EDX measurements.

The balance between silica deposition from the oil phase and the water phase is dependent upon the hydrolysis and condensation rates. By using TMOS instead of TEOS, these rates are significantly increased. Also, in this case, a thin layer of silica is quickly deposited onto the surface of the droplet, tending to encapsulate the droplet. Simultaneously, the rod diameter is reduced, as the remainder of the droplet has a smaller diameter. Because of the higher hydrolysis rate, TMOS is more quickly available for the condensation reaction, but also quickly consumed. Already after a few minutes, the growth front widens again. At this point, TEOS, which can diffuse further into the water droplet before turning to silica, can fill the tube from inside of the droplet. This presses out the water droplet and the growth front widens again.

Another possible explanation for the thinner segment is the consumption of water by the hydrolysis reaction of TEOS, which needs to be replenished from the oil phase. The volume of the water droplet is not large enough to supply the hydrolysis reaction with water for the whole length of the rod. In a "standard" synthesis of rods, the two processes balance to produce rods of uniform thickness. However, a small fraction of silica rods tapers off during growth. The diffusion of water to the droplet then cannot keep up with the consumption by the hydrolysis reaction. However, we believe that the consumption of water by the hydrolysis reaction of TMOS, which is significantly less than the amount of TEOS initially added (1.35 mmol vs 0.27 mmol) is not sufficient to explain such a decrease in diameter. Furthermore, the diameter change was also found for the case of partially hydrolyzed TEOS. Also, TMOS is more likely to hydrolyze already in the pentanol phase and in such a way should not affect the droplet diameter. We therefore propose that the diameter change is caused mainly by the differences in hydrolysis and condensation rates, which promote these processes in the pentanol phase and causes the water-rich droplets to get partially encapsulated. In case the concentration of TMOS, or partially hydrolyzed TEOS, is moderate, the droplets get only partially encapsulated. As growth continues, while maintaining the contact angle at the growth front, the droplet is squeezed to a thread as shown in Figure 9f. The smaller droplet, together with an increased silica growth and changed viscoelastic properties of the droplet, causes the rod growth to be unstable and is likely to be the origin of the change in the growth direction.

CONCLUSIONS

In summary, we have shown that the shape of colloidal silica rods is highly dependent on the growth conditions. The droplets from which they grow were found to be unstable on longer time scales because of Ostwald ripening; the diameter increased dramatically within 24 h. This is caused by the non-zero solubility of water in pentanol, leading to Ostwald ripening. Preparing the emulsions ahead of time should therefore be avoided to improve reproducibility. Because of the non-zero solubility of water and ammonia in pentanol, silica also nucleates there and a population of silica spheres was also found. (As much as 50% of the silica precursor was found to end up as spheres, but for now, this amount was not yet checked for the other conditions where morphology changes for the rod growth were observed). The effect of the hydrolysis rate of TEOS on the rod growth was studied by the partial pre-hydrolysis of TEOS. It was found that the condensation from the continuous phase onto the water droplet−oil interface increased. The addition of partially pre-hydrolyzed TEOS caused a spherical hollow segment to appear at the tip of the rods, which was mentioned earlier in the literature but could not be experimentally proven up to now. The hydrolysis rate of the precursor significantly influences the morphology of the resulting rods (matchstick shape). By tuning the ratio and moment of addition of TMOS or partially hydrolyzed TEOS, one can control the growth precisely. Silica precursors with an increased hydrolysis and condensation rate form silica mainly at the surface of the PVP−water droplet. Silica precursors with a slow hydrolysis and condensation rate likely have time to spread through the droplet before silica forms. Hydrolyzed TEOS and TMOS show a considerable effect on the rod growth. Addition from the start of the synthesis results in silica rods with a hollow sphere at the tip. Delayed addition of TMOS or partial pre-hydrolyzed TEOS results in a thin hollow section which causes a bend in the silica rods. A major difference is the length of the hollow tube: this section is longer in the case of TMOS. Increasing the concentration of TMOS or partially pre-hydrolyzed TEOS increased the bend angle. In conclusion, matchstick silica rods can best be produced using partially hydrolyzed TEOS, whereas for bent silica rods, the angle can be most precisely tuned using TMOS. Producing matchstick particles in a reproducible way is important for instance in studies on particle self-propulsion.[41,57−60] In addition, precise control over the growth of the bent rods is important to be able to study the beautiful bent rod phases, as recently observed in the literature,[48,62] on the single-particle level.

EXPERIMENTAL SECTION

Tuning the Growth of Silica Rods. *Growth Mixture.* The conditions for growth were changed by modifying the steps after the "standard" rod growth procedure. The "standard" growth mixture for silica rods was prepared as follows. First, 1.0 g of PVP (Sigma-Aldrich, M_n = 40 kg/mol) was dissolved in 10.0 mL 1-pentanol (99%, reagent-plus, Sigma-Aldrich). After the PVP had completely dissolved, 1.0 mL of ethanol (100%, Interchema), 0.28 mL of ultra-pure water (Millipore system), and 0.067 mL of aqueous sodium citrate

DOI: 10.1021/acs.chemmater.8b04607
Chem. Mater. 2019, 31, 521−531

dihydrate (0.17 M, 99%, Sigma-Aldrich) were added. After mixing the components, 0.225 mL of ammonia [26.3% (w/w), Sigma-Aldrich] was added. The vial was shaken once more.

"Standard" Silica Rods. In the case of "standard" silica rods, 100 μL of TEOS (98%, Sigma-Aldrich) was added, and the reaction was left to continue overnight without agitation.

Tuning the Hydrolysis Rate of the Silica Precursors. The hydrolysis rate was varied by the addition of TMOS, or by partial hydrolysis of TEOS. The reaction was modified at the start of the synthesis or at intermediate stages. In case the reaction was modified at the start, various amounts of TMOS or partially hydrolyzed TEOS together with TEOS were added at a constant total molar amount of 0.45 mmol. In case the concentration of TMOS was increased, the concentration of TEOS was lowered. In case the growth conditions were modified during the growth, the total molar amount was enlarged to a maximum of 0.54 mmol. First, 100 μL of TEOS (0.45 mmol, 98%, Sigma-Aldrich) was added to the growth mixture, and the reaction was left to continue for 2 h. Then, various amounts of TMOS (≥99%, Sigma-Aldrich) or partially hydrolyzed TEOS were added to the reaction and the vial was carefully homogenized. The reaction product was collected by centrifugation and redispersion steps. The particles were stored in ethanol (100%, Interchema). TMOS was stored at all times in a glovebox (N_2), and the reagent was opened and stored under nitrogen atmosphere. TEOS was used fresh from Sigma-Aldrich and never kept for longer than 1 month. Partially hydrolyzed TEOS was prepared as follows. To 11.0 mL of TEOS (98%, Sigma-Aldrich), 0.8 mL of ultrapure water (Millipore system) and 21.0 μL of concentrated HCl (0.2 mmol, 37%, ACS reagent, Sigma-Aldrich) were added. The vial was shaken vigorously for 10 min. With the addition of 0.01 mmol partially hydrolyzed TEOS, an additional amount of at most 0.057 μmol HCl and 12.8 mmol water were added to the rod growth, which is significantly lower than the molar amount of ammonia (1.7 mmol) and of water (28.6 mmol) already present.

Characterization. The particle morphology was studied using a FEI Tecnai 20 electron microscope operating at 200 kV. Cryogenic TEM was done at a Tecnai 20 using a cryo-TEM holder using BeamSpot 5. The samples were prepared using a FEI vitro-bot: a droplet of 3 μL was place on a Formvar/Carbon film 200 mesh copper grid and blotted twice for 8 s. The grid was immediately plunged into liquid nitrogen and stored in liquid nitrogen.

■ ASSOCIATED CONTENT

Supporting Information

The Supporting Information is available free of charge on the ACS Publications website at DOI: 10.1021/acs.chemmater.8b04607.

Viscosity measurements and cryo-EDX−SEM analysis of matchstick-shaped particles (PDF)

■ AUTHOR INFORMATION

Corresponding Authors

*E-mail: f.hagemans@uu.nl (F.H.).
*E-mail: a.vanblaaderen@uu.nl (A.v.B.).
*E-mail: a.imhof@uu.nl (A.I.).

ORCID

Fabian Hagemans: 0000-0002-4748-8547
Ravi Kumar Pujala: 0000-0001-6905-0434
Arnout Imhof: 0000-0002-7445-1360

Author Contributions

F.H. and R.K.P. authors contributed equally. The manuscript was written through contributions of all authors. F.H., R.K.P., and D.S.H. performed the experimental work under supervision of A.v.B. and A.I. F.H. and D.T.W. performed the viscosity measurements. F.H., M.d.W., and J.D.M. performed the cryo-SEM and cryo-TEM experiments. All authors have given approval to the final version of the manuscript.

Funding

This research is funded by the Netherlands Organisation for Scientific Research (NWO). A.v.B. and R.K.P. acknowledge the European Research Council under the European Union's Seventh Framework Programme (FP/2007-2013)/ERC grant agreement no. [291667].

Notes

The authors declare no competing financial interest.

■ ACKNOWLEDGMENTS

The authors acknowledge Judith Wijnhoven for her contributions to the work on titanium alkoxides and Chris Schneijdenberg for the support with the electron microscopy experiments.

■ ABBREVIATIONS

TEOS, tetraethylorthosilicate; TMOS, tetramethylorthosilicate; PVP, polyvinylpyrrolidone; EDX, energy dispersive X-ray spectroscopy; SEM, scanning electron microscopy; TEM, transmission electron microscopy; FIB, focused ion beam; STEM, scanning transmission electron microscopy

■ REFERENCES

(1) Kuijk, A.; van Blaaderen, A.; Imhof, A. Synthesis of monodisperse, rodlike silica colloids with tunable aspect ratio. *J. Am. Chem. Soc.* **2011**, *133*, 2346−2349.
(2) Blaaderen, A. v. CHEMISTRY: Colloidal Molecules and Beyond. *Science* **2003**, *301*, 470−471.
(3) Duguet, E.; Désert, A.; Perro, A.; Ravaine, S. Design and elaboration of colloidal molecules: An overview. *Chem. Soc. Rev.* **2011**, *40*, 941−960.
(4) Li, F.; Josephson, D. P.; Stein, A. Colloidal assembly: The road from particles to colloidal molecules and crystals. *Angew. Chem., Int. Ed.* **2010**, *50*, 360−388.
(5) Polarz, S. Shape matters: Anisotropy of the morphology of inorganic colloidal particles—Synthesis and function. *Adv. Funct. Mater.* **2011**, *21*, 3214−3230.
(6) Sacanna, S.; Pine, D. J.; Yi, G.-R. Engineering shape: The novel geometries of colloidal self-assembly. *Soft Matter* **2013**, *9*, 8096−8106.
(7) Sacanna, S.; Pine, D. J. Shape-anisotropic colloids: Building blocks for complex assemblies. *Curr. Opin. Colloid Interface Sci.* **2011**, *16*, 96−105.
(8) Sacanna, S.; Korpics, M.; Rodriguez, K.; Colón-Meléndez, L.; Kim, S.-H.; Pine, D. J.; Yi, G.-R. Shaping colloids for self-assembly. *Nat. Commun.* **2013**, *4*, 1688.
(9) Dugyala, V. R.; Daware, S. V.; Basavaraj, M. G. Shape anisotropic colloids: Synthesis, packing behavior, evaporation driven assembly, and their application in emulsion stabilization. *Soft Matter* **2013**, *9*, 6711−6725.
(10) Grzelczak, M.; Pérez-Juste, J.; Mulvaney, P.; Liz-Marzán, L. M. Shape control in gold nanoparticle synthesis. *Chem. Soc. Rev.* **2008**, *37*, 1783−1791.
(11) Fernández-Nieves, A.; Cristobal, G.; Garcés-Chávez, V.; Spalding, G. C.; Dholakia, K.; Weitz, D. A. Optically anisotropic colloids of controllable shape. *Adv. Mater.* **2005**, *17*, 680−684.
(12) Xie, H.; She, Z.-G.; Wang, S.; Sharma, G.; Smith, J. W. One-step fabrication of polymeric Janus nanoparticles for drug delivery. *Langmuir* **2012**, *28*, 4459−4463.
(13) de Folter, J. W. J.; Hutter, E. M.; Castillo, S. I. R.; Klop, K. E.; Philipse, A. P.; Kegel, W. K. Particle shape anisotropy in pickering emulsions: Cubes and peanuts. *Langmuir* **2013**, *30*, 955−964.
(14) Vutukuri, H. R.; Preisler, Z.; Besseling, T. H.; van Blaaderen, A.; Dijkstra, M.; Huck, W. T. S. Dynamic self-organization of side-

DOI: 10.1021/acs.chemmater.8b04607
Chem. Mater. 2019, 31, 521−531

propelling colloidal rods: experiments and simulations. *Soft Matter* **2016**, *12*, 9657−9665.
(15) Manoharan, V. N.; Elsesser, M. T.; Pine, D. J. Dense packing and symmetry in small clusters of microspheres. *Science* **2003**, *301*, 483−487.
(16) Cho, Y.-S.; Yi, G.-R.; Lim, J.-M.; Kim, S.-H.; Manoharan, V. N.; Pine, D. J.; Yang, S.-M. Self-organization of bidisperse colloids in water droplets. *J. Am. Chem. Soc.* **2005**, *127*, 15968−15975.
(17) Yi, G.-R.; Manoharan, V. N.; Michel, E.; Elsesser, M. T.; Yang, S.-M.; Pine, D. J. Colloidal clusters of silica or polymer microspheres. *Adv. Mater.* **2004**, *16*, 1204−1208.
(18) Cayre, O.; Paunov, V. N.; Velev, O. D. Fabrication of dipolar colloid particles by microcontact printing. *Chem. Commun.* **2003**, *18*, 2296−2297.
(19) Cayre, O.; Paunov, V. N.; Velev, O. D. Fabrication of asymmetrically coated colloid particles by microcontact printing techniques. *J. Mater. Chem.* **2003**, *13*, 2445−2450.
(20) Koo, H. Y.; Yi, D. K.; Yoo, S. J.; Kim, D.-Y. A snowman-like array of colloidal dimers for antireflecting surfaces. *Adv. Mater.* **2004**, *16*, 274−277.
(21) Xu, S.; Nie, Z.; Seo, M.; Lewis, P.; Kumacheva, E.; Stone, H. A.; Garstecki, P.; Weibel, D. B.; Gitlin, I.; Whitesides, G. M. Generation of monodisperse particles by using microfluidics: Control over size, shape, and composition. *Angew. Chem., Int. Ed.* **2005**, *44*, 724−728.
(22) Matijevic, E. Uniform Inorganic Colloid Dispersions. Achievements and Challenges. *Langmuir* **1994**, *10*, 8−16.
(23) Yin, Y.; Alivisatos, A. P. Colloidal nanocrystal synthesis and the organic-inorganic interface. *Nature* **2005**, *437*, 664−670.
(24) Gao, J.; Bender, C. M.; Murphy, C. J. Dependence of the Gold Nanorod Aspect Ratio on the Nature of the Directing Surfactant in Aqueous Solution. *Langmuir* **2003**, *19*, 9065−9070.
(25) Liu, B.; Zhang, C.; Liu, J.; Qu, X.; Yang, Z. Janus non-spherical colloids by asymmetric wet-etching. *Chem. Commun.* **2009**, 3871−3873.
(26) Liu, B.; Wei, W.; Qu, X.; Yang, Z. Janus colloids formed by biphasic grafting at a pickering emulsion interface. *Angew. Chem., Int. Ed.* **2008**, *47*, 3973−3975.
(27) Hong, L.; Cacciuto, A.; Luijten, E.; Granick, S. Clusters of amphiphilic colloidal spheres. *Langmuir* **2008**, *24*, 621−625.
(28) Jiang, S.; Chen, Q.; Tripathy, M.; Luijten, E.; Schweizer, K. S.; Granick, S. Janus particle synthesis and assembly. *Adv. Mater.* **2010**, *22*, 1060−1071.
(29) Suzuki, D.; Tsuji, S.; Kawaguchi, H. Janus microgels prepared by surfactant-free pickering emulsion-based modification and their self-assembly. *J. Am. Chem. Soc.* **2007**, *129*, 8088−8089.
(30) Gu, H.; Yang, Z.; Gao, J.; Chang, C. K.; Xu, B. Heterodimers of Nanoparticles: Formation at a Liquid−Liquid Interface and Particle-Specific Surface Modification by Functional Molecules. *J. Am. Chem. Soc.* **2005**, *127*, 34−35.
(31) Böker, A.; He, J.; Emrick, T.; Russell, T. P. Self-assembly of nanoparticles at interfaces. *Soft Matter* **2007**, *3*, 1231−1248.
(32) Sheu, H. R.; El-Aasser, M. S.; Vanderhoff, J. W. Phase separation in polystyrene latex interpenetrating polymer networks. *J. Polym. Sci., Part A: Polym. Chem.* **1990**, *28*, 629−651.
(33) Mock, E. B.; De Bruyn, H.; Gilbert, R. G.; Ramakrishnan, S.; Zukoski, C. F. In Synthesis of anisotropic particles by seeded emulsion polymerization. *AIChE Annual Meeting, Conference Proceedings*. 2005, p 1496.
(34) Kim, J.-W.; Larsen, R. J.; Weitz, D. A. Synthesis of nonspherical colloidal particles with anisotropic properties. *J. Am. Chem. Soc.* **2006**, *128*, 14374−14377.
(35) Park, J.-G.; Forster, J. D.; Dufresne, E. R. High-yield synthesis of monodisperse dumbbell-shaped polymer nanoparticles. *J. Am. Chem. Soc.* **2010**, *132*, 5960−5961.
(36) Nagao, D.; Goto, K.; Ishii, H.; Konno, M. Preparation of asymmetrically nanoparticle-supported, monodisperse composite dumbbells by protruding a smooth polymer bulge from rugged spheres. *Langmuir* **2011**, *27*, 13302−13307.
(37) Kim, J.-W.; Lee, D.; Shum, H. C.; Weitz, D. A. Colloid surfactants for emulsion stabilization. *Adv. Mater.* **2008**, *20*, 3239−3243.
(38) Zhang, J.; Liu, H.; Wang, Z.; Ming, N. Au-Induced Polyvinylpyrrolidone Aggregates with Bound Water for the Highly Shape-Selective Synthesis of Silica Nanostructures. *Chem.—Eur. J.* **2008**, *14*, 4374−4380.
(39) Kuijk, A.; Imhof, A.; Verkuijlen, M. H. W.; Besseling, T. H.; van Eck, E. R. H.; van Blaaderen, A. Colloidal silica rods: Material properties and fluorescent labeling. *Part. Part. Syst. Charact.* **2014**, *31*, 706−713.
(40) Besseling, T. H.; Hermes, M.; Kuijk, A.; de Nijs, B.; Deng, T.-S.; Dijkstra, M.; Imhof, A.; van Blaaderen, A. Determination of the positions and orientations of concentrated rod-like colloids from 3D microscopy data. *J. Phys.: Condens. Matter* **2015**, *27*, 194109.
(41) Longbottom, B. W.; Rochford, L. A.; Beanland, R.; Bon, S. A. F. Mechanistic Insight into the Synthesis of Silica-Based "Matchstick" Colloids. *Langmuir* **2015**, *31*, 9017−9025.
(42) Zhang, A.-Q.; Li, H.-J.; Qian, D.-J.; Chen, M. Kinetically-controlled template-free synthesis of hollow silica micro-/nanostructures with unusual morphologies. *Nanotechnology* **2014**, *25*, 135608.
(43) Dick, K. A. A review of nanowire growth promoted by alloys and non-alloying elements with emphasis on Au-assisted III-V nanowires. *Prog. Cryst. Growth Charact. Mater.* **2008**, *54*, 138−173.
(44) Yu, Q.; Wang, K.; Zhang, J.; Liu, M.; Liu, Y.; Cheng, C. Synthesis of anisotropic silica colloids. *RSC Adv.* **2017**, *7*, 37542−37548.
(45) Murphy, R. P.; Hong, K.; Wagner, N. J. Synthetic control of the size, shape, and polydispersity of anisotropic silica colloids. *J. Colloid Interface Sci.* **2017**, *501*, 45−53.
(46) Hagemans, F.; Vlug, W.; Raffaelli, C.; van Blaaderen, A.; Imhof, A. Sculpting Silica Colloids by Etching Particles with Nonuniform Compositions. *Chem. Mater.* **2017**, *29*, 3304−3313.
(47) Datskos, P.; Sharma, J. Synthesis of segmented silica rods by regulation of the growth temperature. *Angew. Chem., Int. Ed.* **2013**, *53*, 451−454.
(48) Yang, Y.; Chen, G.; Martinez-Miranda, L. J.; Yu, H.; Liu, K.; Nie, Z. Synthesis and Liquid-Crystal Behavior of Bent Colloidal Silica Rods. *J. Am. Chem. Soc.* **2015**, *138*, 68−71.
(49) Sharma, J. Finite-sized One-Dimensional silica microstructures (Rods): Synthesis, assembly, and applications. *ChemNanoMat* **2017**, *3*, 214−222.
(50) Kuijk, A. Fluorescent Colloidal Silica Rods - Synthesis and Phase Behavior. Ph.D. Thesis, Utrecht University, 2012.
(51) Yu, Q.; Wang, K.; Zhang, J.; Liu, M.; Liu, Y.; Cheng, C. Synthesis of anisotropic silica colloids. *RSC Adv.* **2017**, *7*, 37542−37548.
(52) Barton, A. F. M. IUPAC : Solubility data series. In *Alcohols with Water*; Kertes, A. S., Ed.; 1984, Vol. *15*.
(53) von Erichsen, L. Die kritischen Lösungstemperaturen in der homologen Reihe der primären normalen Alkohole. *Brennst.-Chem.* **1952**, *33*, 166−172.
(54) Hagemans, F.; van der Wee, E. B.; van Blaaderen, A.; Imhof, A. Synthesis of Cone-Shaped Colloids from Rod-Like Silica Colloids with a Gradient in the Etching Rate. *Langmuir* **2016**, *32*, 3970−3976.
(55) Donatti, D. A.; Vollet, D. R. Study of the hydrolysis of TEOS-TMOS mixtures under ultrasound stimulation. *J. Non-Cryst. Solids* **1996**, *204*, 301−304.
(56) Datskos, P.; Polizos, G.; Cullen, D. A.; Bhandari, M.; Sharma, J. Synthesis of Half-Sphere/Half-Funnel-Shaped Silica Structures by Reagent Localization and the Role of Water in Shape Control. *Chem.—Eur. J.* **2016**, *22*, 18700−18704.
(57) Morgan, A. R.; Dawson, A. B.; Mckenzie, H. S.; Skelhon, T. S.; Beanland, R.; Franks, H. P. W.; Bon, S. A. F. Chemotaxis of catalytic silica-manganese oxide "matchstick" particles. *Mater. Horiz.* **2014**, *1*, 65−68.
(58) Datskos, P.; Cullen, D. A.; Sharma, J. Step-by-Step Growth of Complex Oxide Microstructures. *Angew. Chem., Int. Ed.* **2015**, *54*, 9011−9015.

DOI: 10.1021/acs.chemmater.8b04607
Chem. Mater. 2019, 31, 521−531

(59) Zhao, B.; Zhou, H.; Liu, C.; Long, Y.; Yang, G.; Tung, C.-H.; Song, K. Fabrication and directed assembly of magnetic Janus rods. *New J. Chem.* **2016**, *40*, 6541−6545.
(60) Gao, Y.; Dullens, R. P. A.; Aarts, D. G. A. L. Bulk synthesis of silver-head colloidal rodlike micromotors. *Soft Matter* **2018**, *14*, 7119−7125.
(61) Livage, J.; Henry, M.; Sanchez, C. Sol-gel chemistry of transition metal oxides. *Prog. Solid State Chem.* **1988**, *18*, 259.
(62) Yang, Y.; Pei, H.; Chen, G.; Webb, K. T.; Martinez-Miranda, L. J.; Lloyd, I. K.; Lu, Z.; Liu, K.; Nie, Z. Phase behaviors of colloidal analogs of bent-core liquid crystals. *Sci. Adv.* **2018**, *4*, No. eaas8829.

DOI: 10.1021/acs.chemmater.8b04607
Chem. Mater. 2019, 31, 521−531